Modeling the Static and Dynamic Behavior of Multi-layer Varistors in the Threshold Voltage Region Depending on the DC Operating Point

Christian Widemann*, Stanislav Scheier**, Stephan Frei**, and Wolfgang Mathis*

* Leibniz Universität Hannover, D-30167, Hanover, Germany
Email: {widemann, mathis}@tet.uni-hannover.de
**Technical University Dortmund, D-44227 Dortmund
Germany, Email: stanislav.scheier@tu-dortmund.de

***Abstract*—In this work, a novel approach to the modeling of ESD protection elements multi-layer varistors (MLV) is presented. Based on measurements of the static I-V-characteristics, an approach similar to the EKV model is used instead of the known ideal I-V-characteristics in the threshold voltage region. Additionally, an equivalent circuit for the representation of the impedance frequency response (especially its low- and mid-frequency behavior) is derived from impedance measurements depending on the varistor's DC operating point. The established model includes frequency depending resistances known from skin effect modeling.**

***Index Terms*—varistor; behavioral modeling; EKV model; skin effect; impedance analysis**

I. Introduction

Electrostatic discharge (ESD) is a severe threat to many integrated circuits (IC). Hence, external protection elements are required to fulfill international standards as well as the specifications of customers. The behavior of the protection elements depend on various factors. Due to the difficulty of measuring the transient voltages and current of the ESD, a deeper metrological insight is often not possible or requires enormous effort. Hence, the efficiency of the protection elements is mostly verified empirically. Simulation-based approaches provide the possibility to foresee the susceptibility to ESD quickly and cost-effectively.

For this purpose, ESD protection elements are often modeled using standard (non-) dynamic devices, i.e. resistances, inductances and capacitances. However, especially deviations between simulation and measurement are observed around the threshold voltage of the varistor. For a better understanding of that effect, a detailed study of the device in frequency domain was carried out. Thus, in [1] an approach based on a hardware description language (HDL) for analog circuits was introduced with which ESD protection elements can be described more flexible. In this work, this approach is continued by means of multilayer varistors (MLV) of type EPCOS CT0603K14G [2]. The necessary steps for the generation of an equivalent model are the same as in [1], namely, determining the static I-V-characteristic and analyzing the impedance frequency response. Nevertheless, in section II, it is shown why for the letter an enhancement of the equivalent circuit model is necessary. The static characteristic of the MLV is determined employing a curve tracer (Keithley 2400) for low currents ($I_{\mathrm{var}} < 50\,\mathrm{mA}$). As shown in section III, the resulting measurements are approximated by different approaches. In section IV, the enhancement for the dynamic behavior is modeled with known skin effect approaches. In combination with these skin effect models, an impedance analysis is performed in section V in order to find the remaining equivalent circuit parameter.

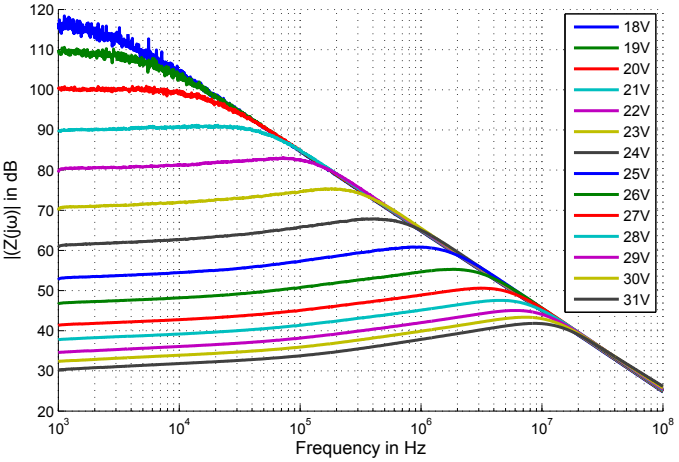

Fig. 1. Impedance frequency response of MLV for various DC bias voltages.

II. Motivation

In contrast to [1], for the measurement of the varistor's frequency response the impedance analyzer *Agilent E5061B* in combination with the *16034G SMD Test Fixture* is employed. By this measurement setup, different DC bias voltages V_{DC} can be applied in addition to the small signal voltage $v_{\mathrm{AC}}(t)$. Consequently, obtained measurement results for different $V_{\mathrm{DC}} = \{17\,\mathrm{V}, 18\,\mathrm{V}, \ldots, 31\,\mathrm{V}\}$ are shown in Fig. 1. It can be observed that the varistor's static resistance (low-frequency

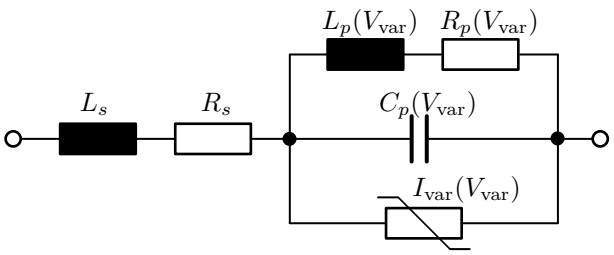

Fig. 2. First approach to an equivalent circuit for the varistor based on impedance analysis.

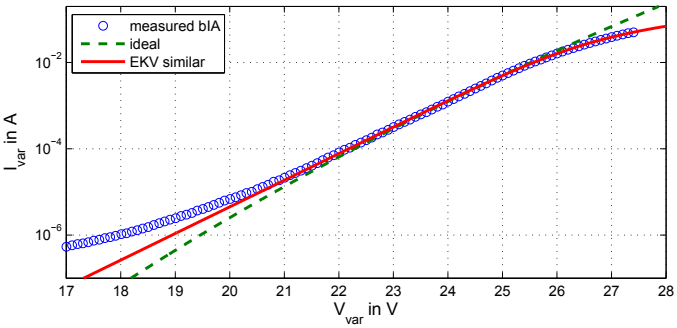

Fig. 3. Approximation of the measured DC characteristics by the two different approaches (1) and (2) with $N = 1$ based on measurements before the impedance analysis.

impedance) decreases for increasing V_{DC} due to its nonlinear I-V-characteristic. However, the frequency response exhibits additionally peaking before the cut-off frequency similar to a weakly-damped resonator. By means of impedance analysis, an equivalent circuit can be found that introduces an additional RL-stage (L_p and R_p, cf. Fig. 2) in parallel to the parasitic capacitance C_p. Nevertheless, the determined values of L_p vary from a few μH to 100 mH. In addition to these rather unphysical values for L_p, the varistor's frequency response shown in Fig. 1 is not constant for low frequencies as it would be for the model in Fig. 2. Hence, in this paper an approach is introduced that uses in addition to linear dynamic elements skin effect modeling (cf. section IV).

III. Approximation of the I-V-characteristics

The first step in modeling the MLV is the determination of the static nonlinear behavior. For this purpose, measurements with the *Keithley 2400* curve tracer are performed. The resulting I-V-characteristics are not described with an analog HDL by look-up tables as it was performed in [1]. Instead, the measurement results are approximated with two different analytic approaches by means of least squares optimization in the threshold voltage region.

A. Ideal varistor characteristic

The first used approach for fitting the measurement results is the idealized power function varistor characteristic of the form

$$I_{\mathrm{var,ideal}} = 1\,\mathrm{A} \cdot \left(\frac{V_{\mathrm{var}}}{V_{1\mathrm{A}}}\right)^{N} \tag{1}$$

that can be found in [3]. In this expression, $V_{1\mathrm{A}}$ states the varistor voltage for that a varistor current of 1 A occurs. The power degree N determines how fast the characteristic increases. If (1) is to describe the negative threshold voltage range as well as the positive without case differentiation, the degree N has to be odd. In [3], a case differentiation for different parts of the I-V-characteristics of the examined ZnO-based varistor is made. Since in this paper the effects in the threshold voltage region are of interest, the measured static characteristic is approximated by means of least squares in the region between 21 V and 28 V. Due to the large value of N the approach (1) is only valid in the threshold region of the varistor. In order to extend the voltage region of validity, another approach similar to the EKV all-region MOS transistor model [4] is utilized.

B. EKV similar approach

As shown in [3] for ZnO-based varistors, the characteristic approach (1) is not suitable for the high voltage region of the varistor characteristic. Since the degree of the power function is very high ($N > 20$ for the regarded CT0603K14G), the function increases to fast for high values of the varistor voltage. Thus, an approach similar to the well-known EKV MOSFET model [4] is applied to varistors in this work for the first time. The function

$$I_{\mathrm{var,EKV}} = I_0 \left[\ln\left(1 + \mathrm{e}^{\frac{V_{\mathrm{var}} - V_0}{V_1}}\right)\right]^{N} \tag{2}$$

for the measured forward current was chosen. In contrast to the actual EKV model equations, here the power degree N is a parameter for the nonlinear least squares approximation that is performed under the constraint of $N \in \mathbb{N}$. For high values of the varistor voltage V_{var} (2) approximates $I_{\mathrm{var}} \propto V_{\mathrm{var}}^{N}$. Since the degree N in (2) is much smaller (normally in the range $2 < N < 10$) than in (1), the high voltage increase is closer to a linear behavior as it is extrapolated in [1] and [3]. Consequently, if the optimization results in $N = 1$, the EKV similar approach (2) covers the high-voltage region of the varistor's characteristics as well. Thus, no further case differentiation is needed. Exemplary approximation results for both approaches are shown logarithmically in Fig. 3.

IV. Skin effect modeling

Since the impedance frequency response for low frequencies is non-constant with a slope $< 20\,\mathrm{dB/decade}$ over several decades and exhibits a peaking close to the cut-off frequency (cf. Fig. 1), the model proposed in [1] has to be extended. However, a first approach with additional network elements such as high-valued a inductance and resistance (cf. Fig. 2 does not model the low-frequency behavior. One possibility for describing the occurring effect, is the skin effect. Due to increasing frequency of the arousing signal the effective cross-section of the electric element decreases to a small surface circular ring with decreasing skin depth [5]. As a result, the resistance of the conductor increases with increasing

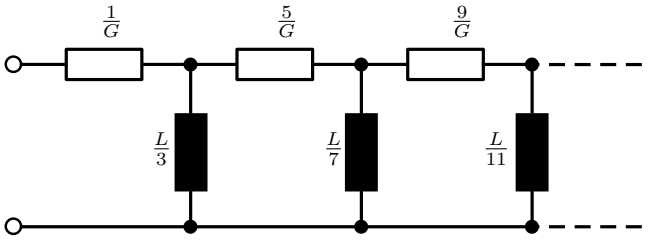

Fig. 4. Ladder network representation of the CFE approach in (5) [6].

frequency. In the following subsections, two possibilities to model the skin effect are regarded that can be found in [6].

A. Series of alternating poles and zeros

The frequency dependent skin effect impedance is commonly modeled with a $\sqrt{s}$ behavior that can be approximated by rational polynomial functions of the type

$$Z_{\mathrm{skin}}(s) = B_1\sqrt{B_2 s} \approx B_1 \frac{\sum_{r=0}^{p} \binom{n+1}{2r}(B_2 s)^r}{\sum_{r=0}^{q} \binom{n+1}{2r+1}(B_2 s)^r} \tag{3}$$

with $p = q = \frac{n}{2}$ for even n and $p = \frac{(n+1)}{2}$ and $q = \frac{(n-1)}{2}$ for odd n [6]. The binomial coefficients depending on the control variable in the sums imply alternating equidistant poles and zeros. A behavioral model for (3) written in Verilog-A can be found in [7]. Therein, two drawbacks of the model using the *laplace_zp* function are named. The number of poles and zeros cannot depend on a parameter, i.e. it has to be a constant. Further, due to the employed *laplace_zp* function, introduced noise cannot be modeled. This is why, a second model for the skin effect is regarded in the following subsection.

B. Continuous fraction expansion

Another model approach to the skin effect is of the form

$$Z_{\mathrm{skin}}(s) = \sqrt{\frac{sL}{G}}\coth\left(sLG\right) \tag{4}$$

$$\approx \frac{1}{G} + \cfrac{1}{\frac{3}{sL} + \cfrac{1}{\frac{5}{G} + \cfrac{1}{\frac{7}{sL} + \cdots}}}. \tag{5}$$

At high frequencies, equation (4) exhibits the $\sqrt{s}$ behavior as well since the $\coth$ saturates to 1. The approximating continuous fraction expansion (CFE) (5) can be realized by a truncated ladder network of the form shown in Fig. 4 [6]. Hence, this model approach can easily be implemented in every circuit simulator. However, in order to gain sufficient accuracy, a great number of stages has to be realized what is very cumbersome. Therefore, a Verilog-A implementation of the n-stage ladder model was developed [8].

V. Modeling the Varistor Impedance

In this work, the focus lies on the modeling of the peaking in the impedance frequency response for several MHz and the non-constant low-frequency impedance. Therefore, in contrast to the model presented in [1], the series inductance that implies in combination with the parallel capacitance C_p a resonance in the GHz-range of the frequency response is neglected. The static varistor characteristic from (1) or (2) in series connection with skin effect impedance $Z_{\mathrm{skin}}(s)$ that can be realized by (3) or (4) the equivalent network in Fig. 5 is considered. In order to determine the circuit parameter depending on the applied V_{var}, based on the impedance approach

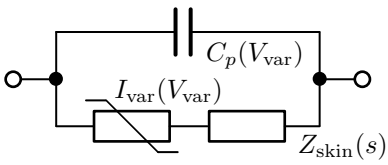

Fig. 5. Equivalent network of the varistor including parasitic low- and mid-frequency effects.

$$Z_{\mathrm{var}}(s) = \frac{r_{\mathrm{diff}} + Z_{\mathrm{skin}}(s)}{sC_p\left(r_{\mathrm{diff}} + Z_{\mathrm{skin}}(s)\right) + 1} \tag{6}$$

a least square approximation of the measured impedance frequency response is performed. In (6) r_{diff} is the differential resistance corresponding to the operating point of the varistor characteristic. In contrast to the circuit parameter of $Z_{\mathrm{skin}}(s)$ and C_p, this resistance is not a optimization parameter in the least squares approximation. Hence, r_{diff} has to be determined in advance.

A. Differential Resistance at DC Operating Point

For the calculation of the differential resistance r_{diff} from the static characteristics (either (1) or (2)), the varistor voltage depending on the DC bias voltage supplied by the impedance analyzer has to be calculated.

Thus, the calculation of the varistor's DC operating point $V_{\mathrm{var}}(V_{\mathrm{DC}})$ is a numerical determination of roots of

$$0 = V_{\mathrm{var}} + 100\,\Omega \cdot I_{\mathrm{var}}(V_{\mathrm{var}}) - V_{\mathrm{DC}} \tag{7}$$

with V_{DC} as a starting point. The $100\,\Omega$ in (7) are the series connection of the source and load resistance of the measurement setup in which the varistor is embedded. Depending on the chosen characteristic $I_{\mathrm{var}}(V_{\mathrm{var}})$ (either (1) or (2)) different DC operating points $V_{\mathrm{var}}(V_{DC})$ are found. As a result, the differential resistance in the DC operating point can be determined with

$$r_{\mathrm{diff}}(V_{\mathrm{DC}}) = \left(\left.\frac{\mathrm{d}I_{\mathrm{var}}}{\mathrm{d}V_{\mathrm{var}}}\right|_{V_{\mathrm{var}}(V_{\mathrm{DC}})}\right)^{-1} \tag{8}$$

that is a constraint for the following least square approximation of the measured impedance frequency response.

B. Calculation of the Model Parameter

In order to determine the unknown equivalent circuit parameter of the varistor model shown in Fig. 5, the magnitude of the impedance frequency response $|Z_{\mathrm{IA}}(f)|$ measured with the impedance analyzer *Agilent E5061B* in combination with the *16034G SMD Test Fixture* is approximated using (6) by means of least squares, i.e. $\min\|\,|Z_{\mathrm{IA}}(f)| - |Z_{\mathrm{var}}(f)|\,\|_2^2$.

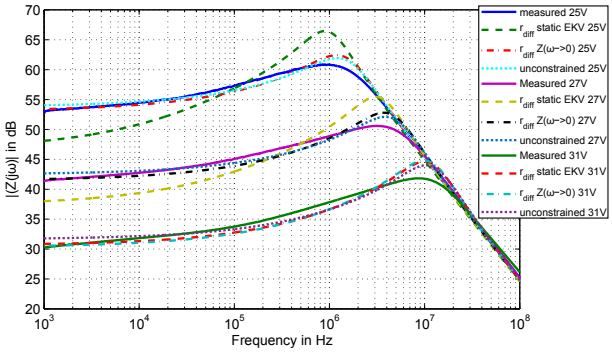

Fig. 6. Approximation of measured impedance frequency response with (6) and (4).

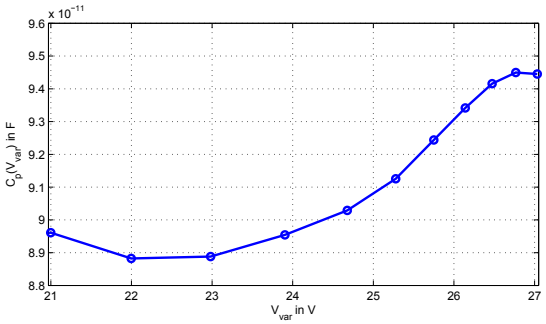

Fig. 7. Parallel capacitance C_p versus varistor's DC operating voltage V_{var}.

In Fig. 6, the approximation results including (4) are shown for different DC bias voltages and choices for r_{diff} in comparison to the measurement results. Due to the fact that the differential resistance is derived from the approximation of static varistor characteristic (8), the optimization using this r_{diff} as a constraint introduces a deviation in the low frequency range. Therefore, to show the possible accuracy of the model in (6), the least squares optimization is executed with the measured $r_{\mathrm{diff}} = Z_{\mathrm{var}}(\omega \to 0)$ and an unconstrained r_{diff}. It is obvious that the model exhibits a similar frequency response as the measurements. However, a perfect match is especially for increasing DC bias voltages not possible.

In Fig. 7 optimization results for C_p that are independent from the choice of r_{diff} are shown versus the varistor's operating voltage calculated from (7) using (2).

The differences between the two different model approaches for the skin effect impedance (3) and (4) are visualized in Fig. 8. Based on the choice $r_{\mathrm{diff}} = Z_{\mathrm{var}}(\omega \to 0)$ the optimization employing (4) leads to parameter L, G for that is $\coth(sLG) \approx 1$ in the regarded frequency range. Hence, the optimization using (3) yield similar results for $B_1\sqrt{B_2}$ that decrease as like $Z_{\mathrm{var}}(\omega \to 0)$ exponentially with V_{var}.

VI. Conclusion

The analysis of the DC bias dependent impedance frequency response revealed that previous circuit models had not been sufficient to describe the examined varistor's low- and mid-frequency behavior. Hence, in addition to the HDL-based model from [1] two possibilities for a frequency dependent

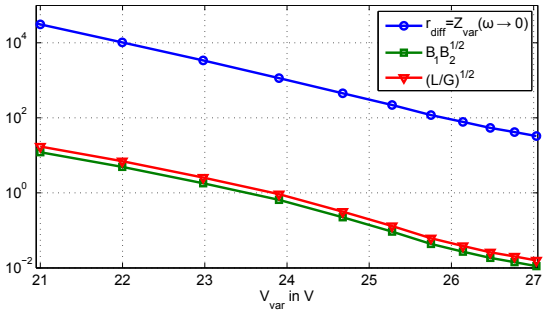

Fig. 8. Comparison of skin effect resistances and the constrained r_{diff}.

resistance as it is known from skin effect modeling were introduced. Consequently, it was shown how the model parameter are calculated by means of least squares approximation in order to fit the varistor's impedance frequency response depending on the applied DC voltage. As a constraint for the optimization problem, the differential resistance of the varistor was applied that can be obtained from the varistor's static characteristics. The latter was measured with a curve tracer and approximated in the varistor's threshold voltage region by two approaches, namely the well-known power function and for the first time an EKV model related approach.

Acknowledgment

This contribution was developed within the scope of the project *Electromagnetic Reliability (EMR) of Electronic Systems for Electro Mobility (EM4EM)* which is funded by the BMBF (Bundesministerium für Bildung und Forschung) under the project number *01M3092K*. The responsibility for this publication is held by the authors solely.

References

[1] B. Arndt, F. zur Nieden, F. Kremer, Y. Cao, J. Edenhofer, and S. Frei, "Modellierung und simulation von esd-schutzelementen mit vhdl-ams," in *EMV-Düsseldorf*, 2010.

[2] EPCOS, *Ceramic transient voltage suppressors SMD multilayer varistor, E series, CT0603K14G*, TDK EPCOS, 2002. [Online]. Available: http://www.epcos.com/inf/75/ds/CT0603K14G.pdf

[3] M. Meshkatoddini, "Investigation of the influence of the zno varistor preparation method on its characteristics," in *Electrical Insulation, 2008. ISEI 2008. Conference Record of the 2008 IEEE International Symposium on*, June 2008, pp. 320–323.

[4] C. C. Enz, F. Krummenacher, and E. A. Vittoz, "An analytical mos transistor model valid in all regions of operation and dedicated to low-voltage and low-current applications," *Analog Integr. Circuits Signal Process.*, vol. 8, no. 1, pp. 83–114, Jul. 1995. [Online]. Available: http://dx.doi.org/10.1007/BF01239381

[5] H. Wheeler, "Formulas for the skin effect," *Proceedings of the IRE*, vol. 30, no. 9, pp. 412–424, Sept 1942.

[6] E. A. Engin, W. Mathis, W. John, G. Sommer, and H. Reichl, "Closed-form network representations of frequency-dependent rlgc parameters," *International Journal of Circuit Theory and Applications*, vol. 33, no. 6, pp. 463–485, 2005. [Online]. Available: http://dx.doi.org/10.1002/cta.330

[7] K. Kundert, *Modeling Skin Effect in Inductors*, 2006. [Online]. Available: www.designers-guide.org/Modeling/ind.pdf

[8] C. Widemann, S. Scheier, W. John, S. Frei, and W. Mathis, "Behavioral modeling and simulation of multi-layer varistors utilizing hardware description languages," in *EMC Europe 2014; Workshop Electromagnetic Reliability (EMR) of Electronic Systems for Electro Mobility*, Gothenburg, Sweden, non-reviewed paper.